Sensors and Materials, Vol. 34, No. 12 (2022) 4737–4753
MYU Tokyo

S & M 3140

Calculation and Comparison of Earthwork Volume Using Unmanned Aerial Vehicle Photogrammetry and Traditional Surveying Method

Suk Bae Lee,[1*] Dongyeob Han,[2] and Mihwa Song[3]

[1]Department of Civil & Infrastructure Engineering, College of Construction and Environmental Engineering, Gyeongsang National University, 33 Dongjin-ro, Jinju, Gyeongsangnam-do 52725, Republic of Korea
[2]Department of Civil Engineering, Chonnam National University, 77 Yongbongro, Bukgu, Gwangju 61186, Republic of Korea
[3]ICT Convergence Research Division, Korea Expressway Corporation Research Institute, 208-96, Dongbu-daero 922 beon-gil, Dongtan-myeon, Hwaseong-si, Gyeonggi-do 18489, Republic of Korea

(Received October 24, 2022; accepted December 19, 2022)

Keywords: UAV photogrammetry, point cloud data, earthwork volume, 3D model, traditional surveying method

Point cloud data obtained by unmanned aerial vehicle (UAV) photogrammetry were used as the basis for creating a 3D model. In this study, we calculated earthwork volume using a 3D model based on such point cloud data at a construction site. An expressway construction site was selected as the study area, and UAV photogrammetry was performed three times, and for comparison purposes, traditional surveying was also conducted the same number of times. Comparison of the earthwork volume calculated by the two methods showed that the volume calculated by UAV photogrammetry was larger in the range of 2.36–2.51% than that obtained by the traditional surveying method (TSM). Therefore, it was found that the method of calculating the earthwork volume at the construction site could be changed to UAV photogrammetry. In addition, comparison of the work efficiency of the two methods showed that UAV photogrammetry in the first work in the study area consumed twice the work time and 1.4 times the work cost over TSM; however, from the second work onward in the study area, the work time and work cost were reduced by approximately half. Therefore, it was found that work efficiency improved as the number of jobs increased.

1. Introduction

The construction industry has three chronic problems: insufficient labor force, low productivity, and high rates of industrial accidents. These points have weakened the competitiveness of the construction industry and have discouraged new engineers from joining the construction industry. Therefore, to overcome these problems, many countries have been making efforts, and smart construction is being proposed as an alternative. Smart construction denotes the lay-out design, construction, and operation of a building or civil infrastructure

*Corresponding author: e-mail: sukbaelee@gnu.ac.kr
https://doi.org/10.18494/SAM4192

ISSN 0914-4935

through collaborative partnerships using digital technologies and industrialized manufacturing techniques to improve productivity and sustainability, minimize the whole life cost, and maximize user benefits. In the design phase, smart construction software allows organizations to review the lay-out design and ensure that factory and on-site operations are planned and optimized in a way to guarantee the best health, welfare, and safety outcomes.[1] Smart construction is being promoted in Korea with three goals: first, improving construction productivity by 50%, second, improving safety by reducing the death rate per 10000 people from 1.66 to 1.0, and third, initiating/promoting 500 high-value-added startups. In addition, the roadmap for promoting smart construction includes features such as unmanned aerial vehicle (UAV) photogrammetry, 3D building information model (BIM) design, and facility maintenance by digital twin.[2] However, the common basis of facility maintenance through UAV photogrammetry, 3D BIM design, and digital twin is point cloud data. UAV photogrammetry is particularly recognized as the most economical and efficient way for mapping using orthophoto mosaics and digital surface models (DSMs).[3–9] UAV photogrammetry is a surveying technique that enables generating point clouds, 3D surface models, and orthophoto mosaics.[5,6] Unmanned aerial systems (UAS) have various applications on construction sites. They provide a bird's-eye view for supervising construction site personnel as well as providing live feedback on actions taking place on-site.[10] Lee *et al.* found that UAV photogrammetry can also create contour lines using a plotter based on stereoscopic vision similarly to traditional photogrammetry.[11] In addition, UAV photogrammetry can quickly monitor disasters; thus, many studies have been conducted to create topography where landslide has occurred and to evaluate displacement.[12–16] To utilize UAV photogrammetry in the construction site, studies on DEM production based on point cloud data[17,18] and studies to calculate the earthwork volume were conducted.[19–22] In addition, a study on detecting changes using a 3D model or orthoimage created periodically for a construction site has also been conducted.[23]

In this study, we aimed to verify whether accurate earthwork volume can be calculated using UAV photogrammetry in the construction site. This method can greatly reduce the work and cost of calculating the earthwork volume at the construction site, which is usually performed by the traditional surveying method (TSM). For this study, an expressway construction site was selected as the study area, and UAV photogrammetry was performed three times over three months, and the earthwork volume was calculated. For comparison, the earthwork volume was also calculated by TSM at nearly the same time every month.

This paper is organized as follows. The research background, research objectives, and previous studies are introduced in Sect. 1, and the two methods used in the study, namely, UAV photogrammetry and TSM, are introduced in Sect. 2. The experimental results obtained by the two methods in the study area are presented in Sect. 3; the results are discussed from a technical perspective in Sect. 4, and finally, the major findings of this study are summarized in Sect. 5.

2. Materials and Methods

To calculate the amount of earthwork when designing or constructing roads in Korea, first, longitudinal and cross-sectional surveys are conducted in the direction of the road center line

and for each chain at 20 m intervals, respectively. Second, longitudinal sectional and cross-sectional drawings are created on the basis of these surveying results; third, the amount of earthwork is calculated by averaging both the sections with neighboring sections. In this study, we aim to verify whether earthwork volume can be calculated reliably from 3D models constructed using UAV photogrammetry. For this study, a 500 m length of Section 2 of the Gangjin-Kwangju Expressway construction site was selected as the study area, and the earthwork volume was calculated from the 3D model built using UAV photogrammetry. In addition, to compare and verify the measured earthwork volume, traditional surveying was first conducted in the study area to measure the earthwork volume. Our selected study area was an embankment section; therefore, the earthwork volume here refers to the embankment volume.

2.1 Study area

The study area was a part of Section 2 of the Gangjin-Kwangju Expressway Route 255 construction site, being constructed by the Korea Expressway Corporation. The finished Expressway Route 255 between Gangjin and Kwangju is expected to be 51.11 km long and 23.4 m wide (four lanes); the construction started in 2017 and is expected to end in 2024. The expressway comprises seven sections in total, with Section 2 covering a length of 7.84 km. The selected study area for earthwork volume calculation covered a 500 m section from Station 7 + 600 to Station 8 + 100, where the earthwork was actively progressing. Figure 1 shows the location of the study area.

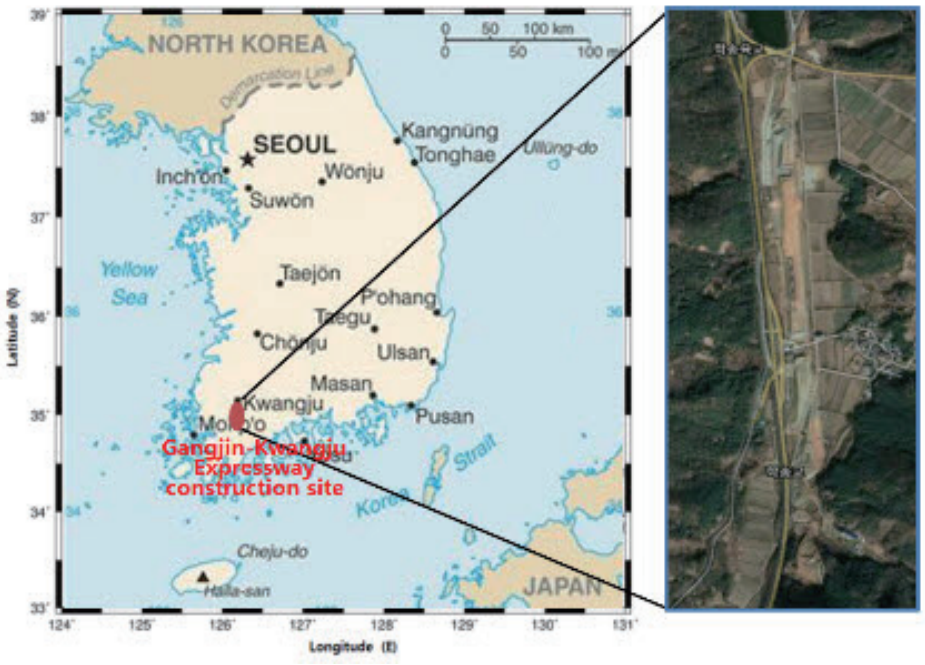

Fig. 1. (Color online) Location of study area, part of the Gangjin-Kwangju Expressway Route 255 construction site in Korea.

2.2 UAV photogrammetry

Figure 2 shows the procedures and methods for calculating earthwork volume by UAV photogrammetry.

2.2.1 Planning

In this planning stage, the works such as setting of the flying area to perform UAV photogrammetry, the selection of drones, the procedure for obtaining filming permission and flight approval, the arrangement of ground control points (GCPs) and check points (CPs), and the field check were performed. In the field check process, the elements of flight obstacles, radio interference elements, and drone take-off and landing sites in the filming area were checked. In this study, a fixed-wing drone, Swiss Sensefly's eBee Plus, was selected because of its efficiency in large-scale construction sites. This drone weighs 1.1 kg, spans 110 cm, has a maximum flight time of 59 min, and supports real-time kinematic (RTK) and postprocessing kinematic (PPK) Global Navigation Satellite System (GNSS) positioning functions. Equipped with an anemometer and ground sensors, it can automatically return if it encounters a strong wind speed (more than 12 m/s) during flight, and can take evasive action through automatic elevation rise after detecting an obstacle. The RGB sensor resolution is 20 MP. Pix4D mapper and Virtual Surveyor software programs were used for processing the captured images.

2.2.2 Establishment of air-photo signal and GCP surveying

UAV photogrammetry was performed in accordance with the "UAV Survey Work Regulations" of the Korean National Geographic Information Institute. First, air-photo signals

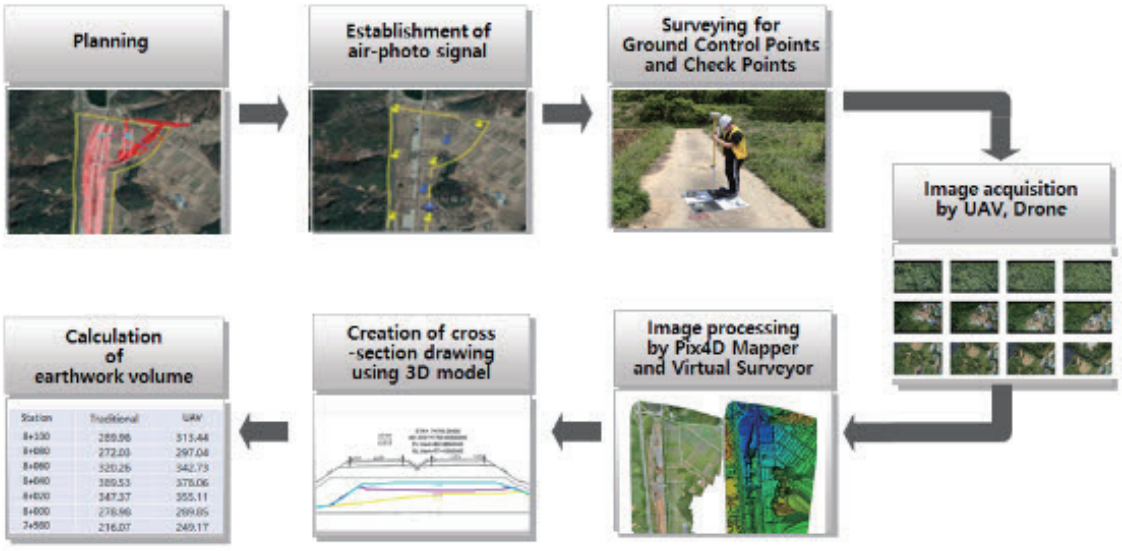

Fig. 2. (Color online) Procedures and methods for calculating earthwork volume by UAV photogrammetry.

were installed at ten GCPs and four CPs, and GCP surveying was performed using the GNSS Network-RTK, Virtual Reference Station (VRS). Table 1 shows the 3D coordinates of all GCPs and CPs, which are the Transverse Mercator (TM) projection coordinates based on the world geodetic system in Korea.

2.2.3 Image acquisition

The UAV flights were operated three times every month, as shown in Table 2. The GSD was aimed at 4 cm, and in the first UAV flight, 884 images were acquired, which was the sum of two flights divided into longitudinal and transverse directions. In the second and third UAV flights, 414 and 393 images were acquired, respectively. The reason for conducting UAV flights thrice is to calculate the amount of earthwork generated every month.

2.2.4 Image processing

Images obtained through three UAV flights over the study area were processed to create orthomosaics and DSMs. Figures 3 and 4 show the three generated orthomosaics and DSMs, respectively, obtained from the three UAV flights over the study area. Pix4DMapper software

Table 1
3D TM coordinates at GCPs and CPs achieved by GNSS survey.

Division	Number	*X*	*Y*	*Z*
Ground control point	GCP 01	176168.668	242968.826	52.382
	GCP 02	176502.657	242977.317	50.616
	GCP 03	176354.447	242563.505	53.724
	GCP 04	176206.723	242521.202	58.435
	GCP 05	176240.962	242158.519	70.086
	GCP 06	176377.472	242139.595	60.895
	GCP 07	176294.477	241531.150	81.694
	GCP 08	176418.952	241668.432	73.298
	GCP 09	176288.34	241305.975	90.085
	GCP 10	176390.588	241419.308	86.114
Check point	CP 01	176453.147	242734.087	51.816
	CP 02	176366.114	242351.056	55.919
	CP 03	176272.714	241785.720	76.533
	CP 04	176354.677	241509.119	81.061

Table 2
Overview of UAV photogrammetry performed in this study.

UAV flight date	GSD (cm)	Overlap ratio	Area coverage (km^2)	Flight time (min)	Number of images
Apr 28, 2020	First: 3.97 Second: 4.34	Long 80% Side 70%	1.251	67	First 476 Second 408 Subtotal 884
May 28, 2020	3.91	Long 80% Side 70%	1.105	42	414
Jul 2, 2020	3.88	Long 70% Side 70%	1.066	36	393

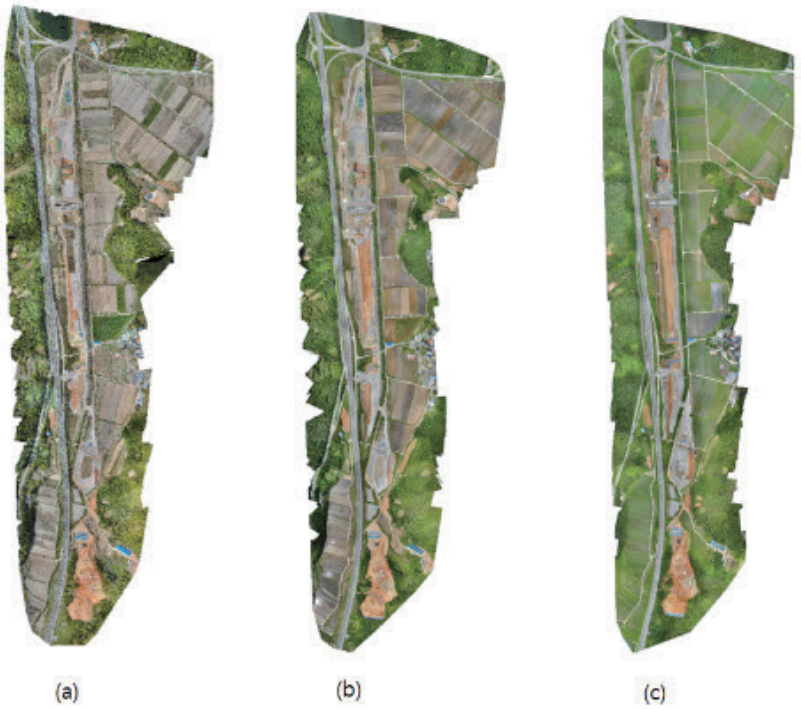

Fig. 3. (Color online) Generated orthomosaics over the study area: (a) first, (b) second, and (c) third.

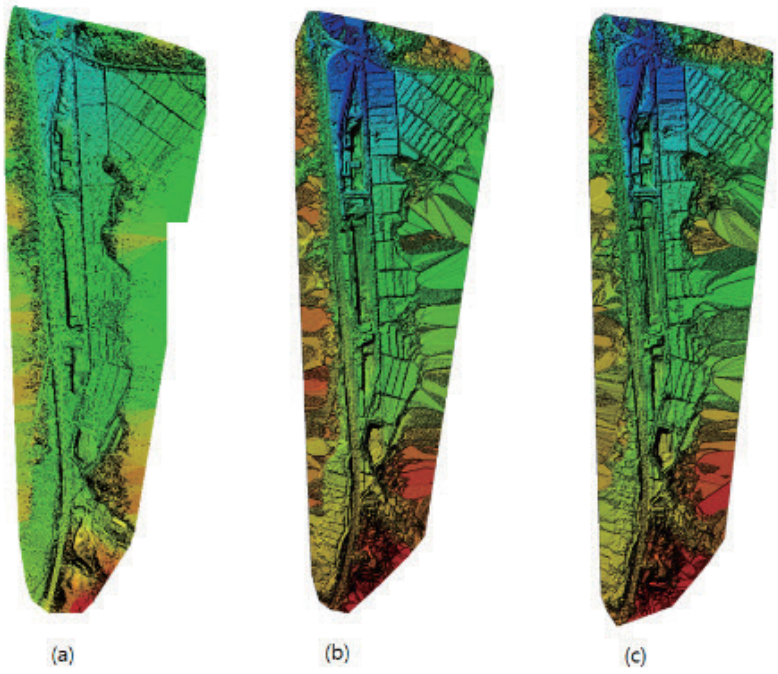

Fig. 4. (Color online) Generated DSMs over the study area: (a) first, (b) second, and (c) third.

was used for this work. A 3D model of the study area was created using the orthomosaics and DSMs. To create a 3D model, the longitudinal and transverse directions were photographed at

double height, and the shaded area was minimized through tilting photography. For the production of realistic 3D models, Context Capture software that can produce high-quality 3D models and supports various output formats was used. Table 3 shows the accuracy of the orthomosaics and DSMs evaluated in CPs. Since the coordinates of GCPs are input to the image during the Aerial Triangulation (AT) process, it cannot show the exact difference. Therefore, the accuracy was evaluated with the CPs that were not input to the AT process. As a result of the evaluation, the root mean square error (RMSE) of the residuals of the plane coordinates of X and Y showed a distribution from 2.0 to 5.5 cm, and the RMSE of height is from 5.0 to 9.3 cm, indicating a larger difference than the plane.

2.3. TSM

In this step, the earthwork volume was calculated using TSM to compare it with that calculated by UAV photogrammetry. Figure 5 shows the procedures and methods for calculating

Table 3
Accuracy of the aerial triangulation process at CPs (unit: m).

Division	First work			Second work			Third work		
	ΔX	ΔY	ΔZ	ΔX	ΔY	ΔZ	ΔX	ΔY	ΔZ
Minimum	0.024	0.002	0.025	0.014	0.009	0.012	0.006	0.013	0.0004
Maximum	0.047	0.075	0.067	0.037	0.061	0.176	0.060	0.105	0.177
Mean	0.012	0.018	0.017	0.026	0.016	0.052	0.017	0.019	0.058
RMSE	0.029	0.044	0.050	0.027	0.032	0.093	0.033	0.055	0.091

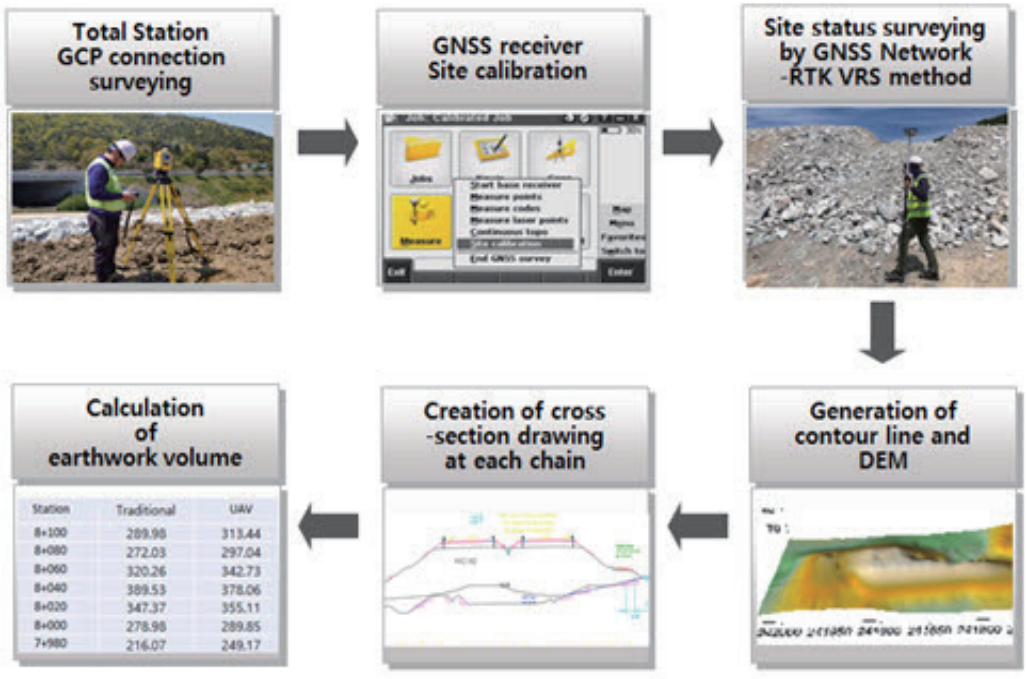

Fig. 5. (Color online) Procedures and methods for calculating earthwork volume by TSM.

earthwork volume by TSM. TSM involves conducting longitudinal and cross-sectional surveys using a total station and a GNSS receiver. Longitudinal surveying refers to surveying the height in the direction of the road center line, and cross-sectional surveying refers to surveying the height at the point where the elevation changes in the transverse direction in each chain. Then, a longitudinal sectional drawing and a cross-sectional drawing are created on the basis of these longitudinal and cross-sectional surveying results, and the earthwork volume can be calculated.

For traditional surveying, not only the coordinates of the ten GCPs conducted for UAV photogrammetry were utilized, but also new several control points were made and connected to the GCPs with a Trimble RTS 773 total station. New control point coordinates were used to calibrate the GNSS survey. In the network-RTK VRS survey, after performing site calibration, the local coordinate system was configured and the current status surveying was performed on the construction site using the Trimble R10 GNSS receiver. Table 4 shows the number of survey points acquired with the network-RTK VRS surveying method and the survey date. On the basis of the current status survey points, the nearest neighbor method was used to interpolate and create a contour line for the study area using Surfer 9.0 software. Three contour line drawings and 3D road DEMs created by using TSM are shown in Figs. 6 and 7, respectively. In principle, the TSM was performed on the same date as the UAV photogrammetry, but a small time difference occurred because of the schedule of heavy equipment use at the construction site.

Table 4
Overview of TSM performed in this study.

Order	Surveying date	Number of survey points
First	Apr 28, 2020	1344
Second	May 27, 2020	628
Third	Jun 30, 2020	463

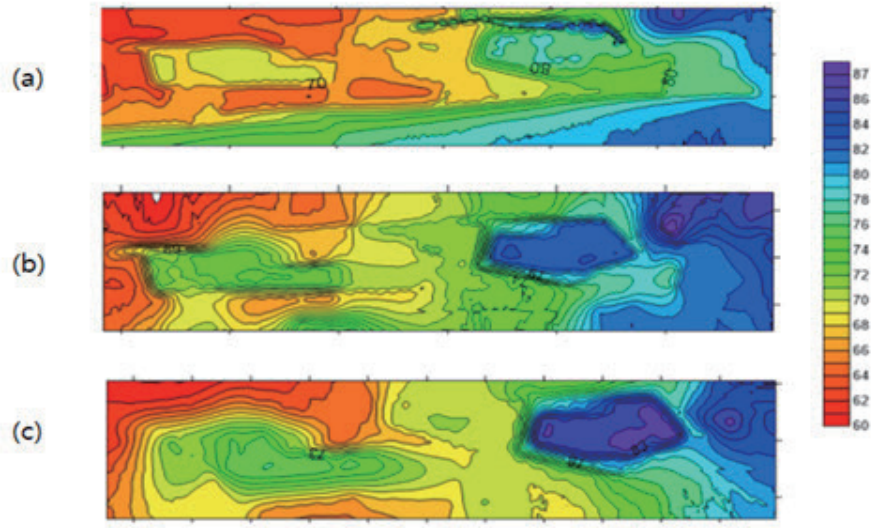

Fig. 6. (Color online) Three contour line drawings created by TSM: (a) first, (b) second, and (c) third.

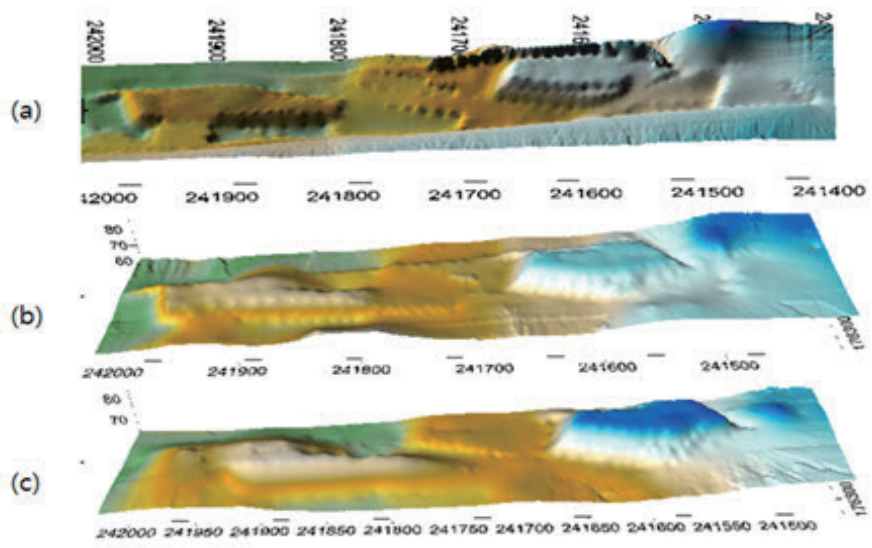

Fig. 7. (Color online) Three 3D road DEMs created by TSM: (a) first, (b) second, and (c) third.

3. Results

3.1. Calculation of earthwork volume using 3D model of UAV photogrammetry

In this step, the earthwork volume was calculated using the 3D model obtained by UAV photogrammetry. The earthwork volume can be calculated directly from the 3D model, but for accurate comparison with TSM, a cross-sectional drawing was created for each station (chain), and the earthwork volume was calculated by averaging both sections. Figure 8 shows the steps from the 3D model to cross-sectional drawing creation. First, a modified 3D model was created by removing artificial objects from the 3D model in Fig. 8(a). In Fig. 8(b), the road center line was superimposed on the modified 3D model, in Fig. 8(c), the cross-sectional line was superimposed on the modified 3D model, and in Fig. 8(d), the current height line was extracted from the entire cross section. Virtual Surveyor and Civil Pro software were used for this step. The cross-sectional drawing of each station was created by superimposing it on the road CAD design drawing provided by the Gangjin-Kwangju Construction Project Office to understand the progress of the construction, and the cross-sectional drawing of Station 7 + 700 is shown in Fig. 9 as the sample. The ground line and road plan line are shown in black on the CAD design drawing, and the primary survey results obtained by UAV photogrammetry are shown in yellow, the secondary survey results are shown in purple, and the third survey results are shown in light blue. The earthwork volume was calculated as shown in Eq. (1) using the averaging method for both sections. The height of the road center line of each station was also extracted from the modified 3D model. Figure 10 shows the height change of the road center line and Figure 11 shows the area change of the cross section at each station.

$$V = \frac{1}{2}(A1 + A2)L \tag{1}$$

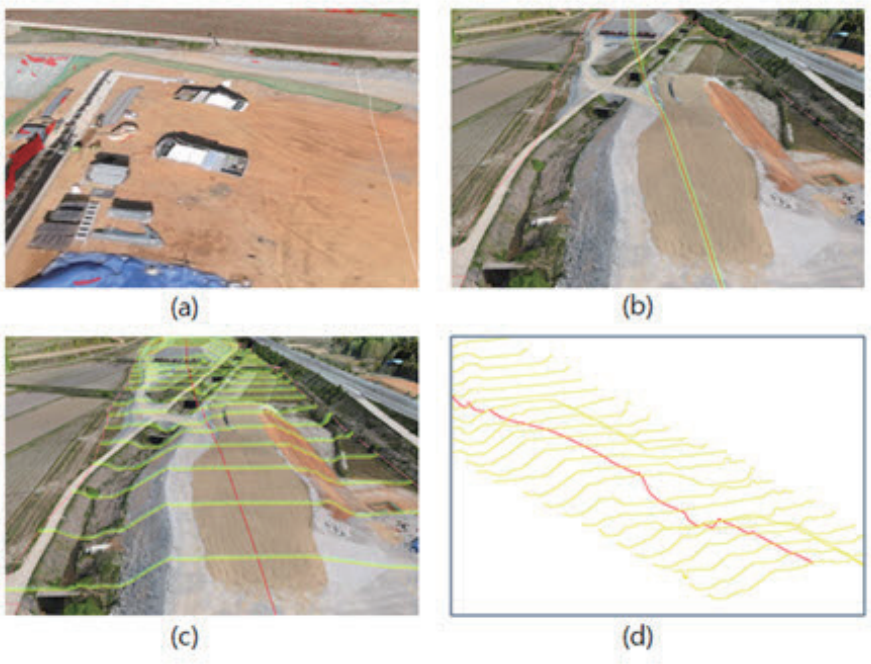

Fig. 8. (Color online) Procedure to obtain cross-sectional drawing from 3D model. (a) Remove artificial object from the 3D model. (b) Overlay the road center line on the 3D model. (c) Overlay each cross-sectional line on the 3D model. (d) Extract the current height line of all the cross sections.

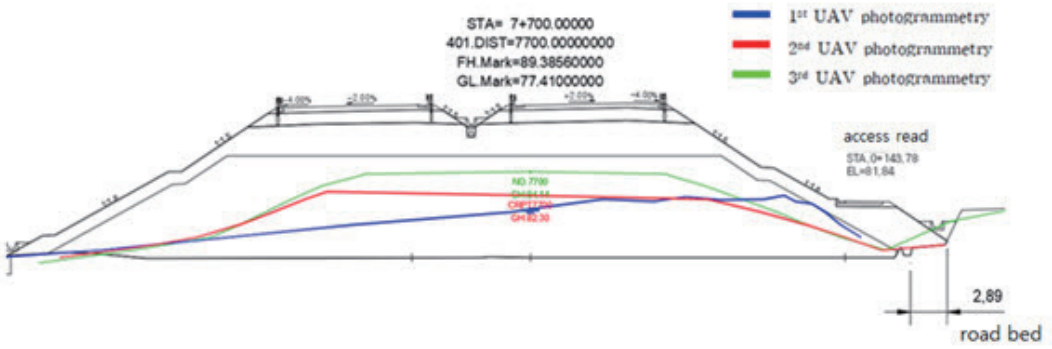

Fig. 9. (Color online) Three different-colored cross-sectional height lines obtained from three UAV photogrammetry flights were superimposed on the road CAD design drawing on station 7 + 700.

Here, V is the earthwork volume, A_1 and A_2 are the cross-sectional areas of both sections, and L is the distance between the two adjacent sections.

3.2 Calculation of earthwork volume by TSM

In TSM, the generated 3D road DEM was used to create a cross-sectional drawing of each station and calculate the earthwork volume. The cross-sectional drawing of each station was created by superimposing it on the road CAD design drawing provided by the Gangjin-Kwangju

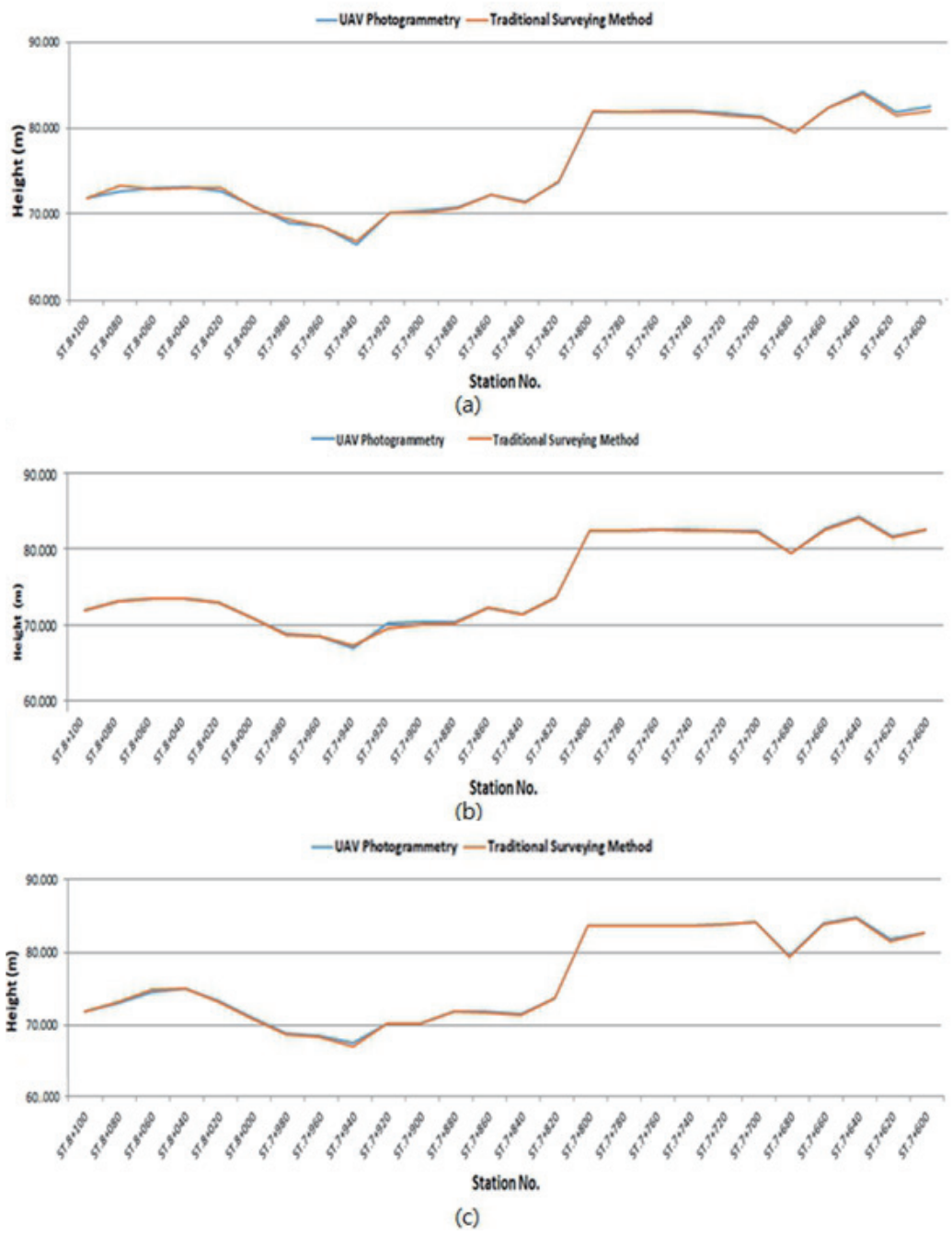

Fig. 10. (Color online) Comparison of center line height: (a) first work, (b) second work, and (c) the third work at each station determined by the two methods.

Construction Project Office to understand the progress of the construction, and the cross-sectional drawing of Station 7 + 700 is shown in Figure 12 as a sample. In the road CAD design drawing, the ground line and road plan part are shown in black, the first surveying result in blue, the second surveying result in red, and the third surveying result in green. Therefore, the area of

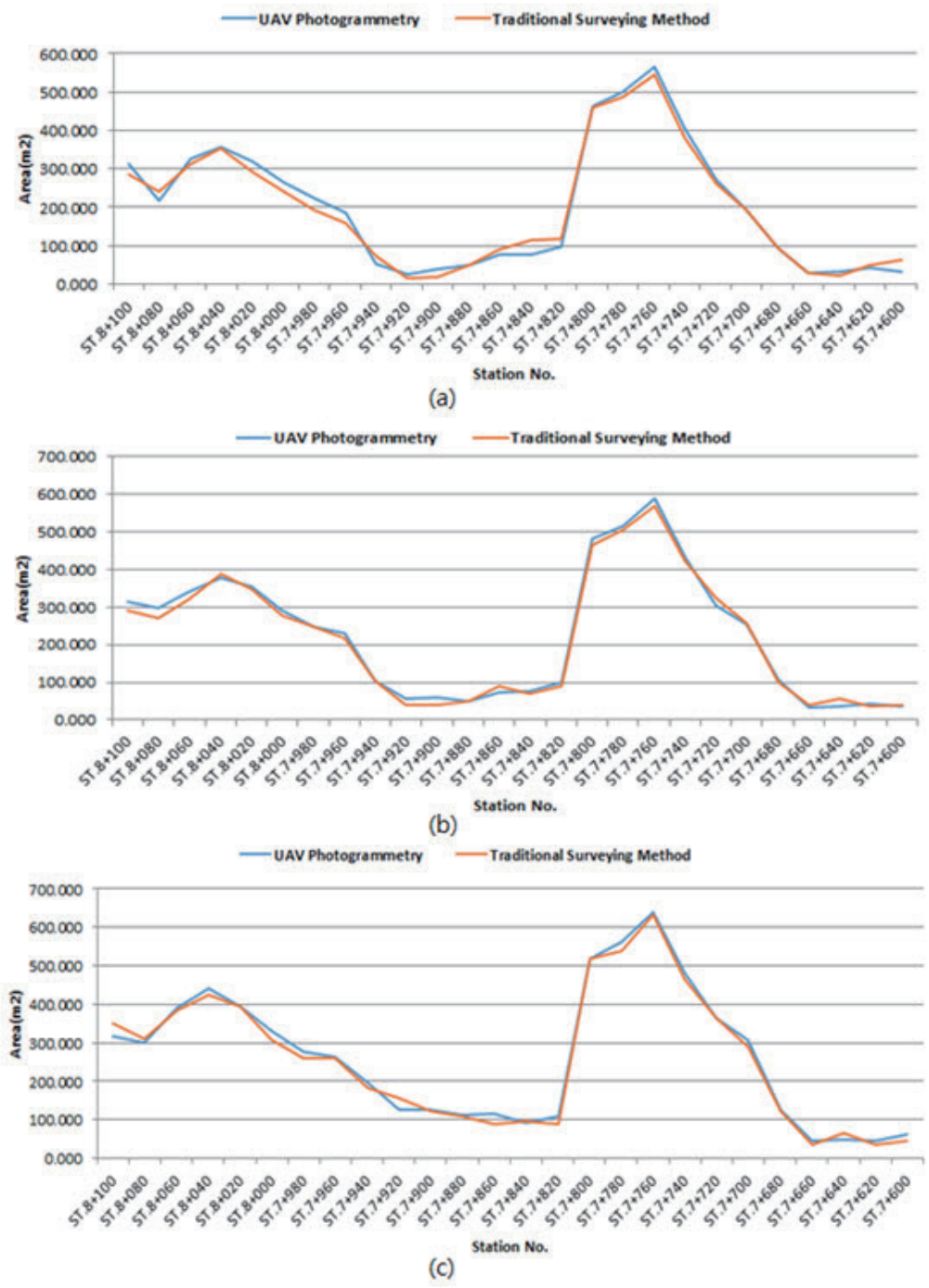

Fig. 11. (Color online) Comparison of cross-sectional area: (a) first work, (b) second work, and (c) third work at each station determined by the two methods.

polygonal cross sections according to each measurement result was calculated using Smart Construction software, and the earthwork volume was calculated using the averaging method for both sections. The height of the road center line at each station was extracted from the 3D road

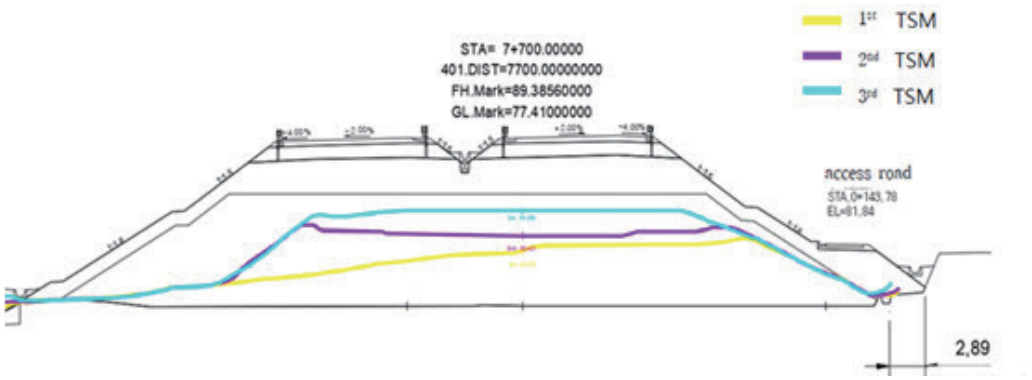

Fig. 12. (Color online) Three different-colored cross-sectional height lines obtained from three traditional surveying results were superimposed on the road CAD design drawing on Station 7 + 700.

DEM. Figure 10 shows the height change of the road center line and Figure 11 shows the area change of the cross section at each station.

3.3. Comparison of earthwork volume calculated by the two methods

Table 5 shows the results of calculating the earthwork volume using the two methods. As shown in Table 5, the earthwork volumes calculated by UAV photogrammetry were 101692, 112753, and 132134 m^3 in the first, second, and third works, respectively. The earthwork volumes calculated by TSM were 99294, 109919, and 128959 m^3 in the first, second, and third works, respectively. Therefore, comparison of the calculated earthwork volumes showed that the UAV photogrammetry results exceeded those of the TSM by 2398 m^3 (2.36%), 2834 m^3 (2.51%), and 3255 m^3 (2.46%) in the first, second, and third works, respectively.

In addition, the comparative result of measuring the road center line height by the two methods three times is shown in Fig. 10, and that of the cross-sectional area measured three times is shown in Fig. 11. As shown in Fig. 10, the road center line heights obtained by the two methods are almost the same. However, the results at ST. 8 + 080 and ST. 7 + 600, ST. 7 + 920, and ST. 7 + 940 in the first, second, and third works, respectively, were slightly different. Comparison of the cross-sectional areas in Fig. 11 showed that there were a few differences from ST. 8 + 080 to ST. 7 + 802 in the first work, ST. 7 + 920 to ST. 7 + 860 in the second work, and in ST. 8 + 100, ST. 7 + 920, and ST. 7 + 780 in the third work. However, it was found that the earthwork volume obtained by UAV photogrammetry was consistently higher (2.36 to 2.51%) than that obtained by TSM.

Table 5
Earthwork volume calculated by the two methods.

Method	First work (m^3)	Second work (m^3)	Third work (m^3)
UAV photogrammetry (A)	101692	112753	132134
TSM (B)	99294	109919	128959
Difference (A−B)	2398 (2.36 %)	2834 (2.51 %)	3255 (2.46 %)

4. Discussion

As shown in Table 5, the earthwork volume calculated in this study using point cloud data obtained by UAV photogrammetry was consistently larger (from 2.36 to 2.51%) than that obtained by TSM. After analyzing the cause, we found that natural or artificial objects are not completely removed when creating DEMs or 3D models in DSM in data processing software. In addition, when there is a 3D structure at the construction site, the edge part is not accurately recognized. Therefore, the overlapping ratio of the image should be sufficiently high, and double image acquisition at different flight heights is recommended to accurately recognize the 3D structure. If bridges are present at the construction site, it isconsidered that a LiDAR survey performed in parallel with UAV photogrammetry can produce a good 3D model without shadow areas. As shown in Table 5, subtracting the second work from the third work or subtracting the first work from the second work can provide an estimate of the earthwork completed within a month. Therefore, by using orthomosaics and 3D models constructed using UAV photogrammetry on the basis of these results, we can track the progress of the earthwork at the construction site. Figure 13 shows the possibility of (a) earthwork volume management using a cross-sectional view, (b) overlapping management with constructed slopes and design drawings, and (c) calculation of slope germination area using orthomosaics and 3D models. Therefore, it is expected that if the 3D BIM design drawing, which is a key component of smart construction, is superimposed on the 3D model made with point cloud data, it will help easily recognize the areas where the construction has progressed or is still pending and will also ease the process management.

To compare the work efficiency of the two methods, the working technicians were asked to fill out the resource input survey form, in which the grade and name of the engineer and the work start and end times are recorded to determine the number of technicians utilized and their work duration. Table 6 shows the time and cost invested in the work based on the resource input survey entries. The cost was calculated by multiplying the invested engineers' working man-days with the 2020 engineering wages announced by the Korea Engineering Association. As shown in Table 6, comparison of the first, second, and third works showed that UAV photogrammetry consumed approximately four times the input time and a little more than four

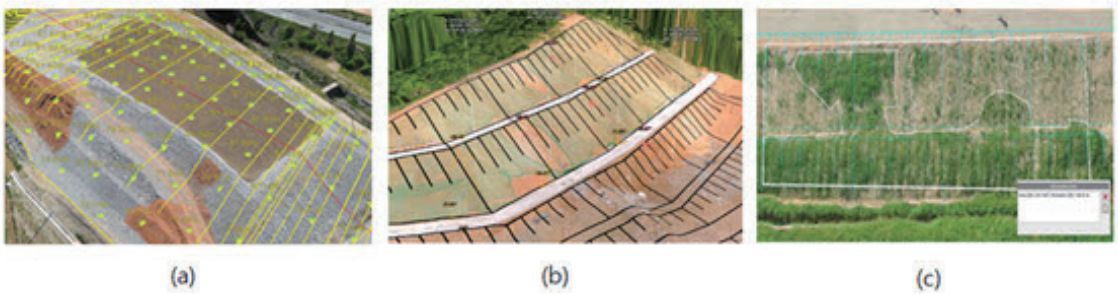

Fig. 13. (Color online) (a) Earthwork volume management using a cross-sectional view, (b) overlapping management with constructed slopes and drawings, and (c) calculation of slope germination area using orthomosaic and 3D model.

Table 6
Comparison of working hours and cost between the two methods.

Working time	Division	UAV photogrammetry	TSM
First work (April 2020)	Working hours (h)	181.0	96.0
	Working cost	4472 USD (4958296 KRW)	3157 USD (3500219 KRW)
Second work (May 2020)	Working hours (h)	41.0	79.0
	Working cost	1251 USD (1387596 KRW)	2041 USD (2262768 KRW)
Third work (July 2020)	Working hours (h)	46.5	96.0
	Working cost	1276 USD (1414262 KRW)	2812 USD (3118572 KRW)
Total	Working hours (h)	268.5	271
	Working cost	6999 USD (7760114 KRW)	8010 USD (8881559 KRW)

times the work cost in the first work compared with those in the second and third works. However, in the case of TSM, the work time decreased by 16 h and the work cost decreased by approximately 902 USD (1 million KRW) in the second work compared with the first and third works, but it did not change significantly.

In addition, comparison of UAV photogrammetry and TSM showed that their overall working hours were similar and the work cost by the UAV photogrammetry decreased by 13.6% compared to the TSM. However, the first work with UAV photogrammetry consumed twice as much work time and 41.6% more work cost than with TSM. This is because GCP surveys were conducted directly at all GCPs and CPs to comply with the "Unmanned Air Vehicle Surveying Work Regulations" of NGII. If this GCP survey is omitted by using a UAV capable of GNSS PPK, the work time and cost may be significantly reduced. However, these earthwork volume data were compiled by measuring the construction site three times for three months. Assuming that such surveys were performed similarly for all the months of the year, UAV photogrammetry would have consumed 662.25 h of work and cost 18,370 USD (20368475 KRW). In addition, TSM would have consumed 1058.5 h and cost 29,850 USD (33097589 KRW). Therefore, assuming that the expressway construction site performed the same work every month, UAV photogrammetry reduces the work time by 396.25 h compared with TSM in one year, resulting in a 37.4% efficiency improvement, and it is expected that a reduction of 11480 USD (12729114 KRW) could lead to a budget saving of 38.5%.

5. Conclusions

In this study, we used UAV photogrammetry to calculate earthwork volume. An expressway construction site was selected as the study area, and three UAV photogrammetry and traditional surveys were conducted. After analyzing the results, the following conclusions were obtained.

First, it is possible to create a 3D model of a construction site using point cloud data and orthogonal images acquired by UAV photogrammetry, based on which cross-sectional drawings can be produced and the earthwork volume can be calculated. In addition, when the earthwork volume calculated by this method was compared with that calculated by TSM, there was no significant difference, which indicated that the earthwork volume based on point cloud data acquired by UAV photogrammetry at the construction site is reliable. However, to calculate the

amount of earthwork without such a small error, it is recommended to use a LiDAR sensor in addition to the RGB sensor.

Second, if the created cross-sectional drawing based on the point cloud data overlaps with the cross-sectional 2D road design drawing, it is evident that the progress of the construction can be easily tracked and can be used for process management. This means that when a 3D BIM design drawing is created for a construction site, a 3D model based on point cloud data can be overlaid, making it a tool to easily track the construction progress.

Third, today, at construction sites, TSM is performed monthly to calculate the completed earthwork volume, and the result is used as basic data for calculating the work cost. However, it has been shown that changing from TSM to UAV photogrammetry can increase the efficiency in terms of work time and cost by more than 30%.

Acknowledgments

This work was supported by Gyeongsang National University, University Accounting Sabbatical Support in 2021. We would also like to thank the Gangjin-Kwangju Expressway Construction Project Office for not only providing 2D CAD design drawings but also cooperating to enable UAV photogrammetry and traditional surveying at the expressway construction site.

References

1 Smart Construction A Guide for Housing Clients, https://www.constructionleadershipcouncil.co.uk/wp-content/uploads/2018/10/181010-CLC-Smart-Construction-Guide.pdf (accessed 29 August 2022).
2 Ministry of Land Infrastructure and Transportation, Korea: Smart Construction Technology Roadmap for Innovation in Construction Productivity and Enhancement of Safety (2018) p. 9.
3 I. Colomina and P. Molina: ISPRS J. Photogram. Remote Sens. **92** (2014) 79. https://doi.org/10.1016/j.isprsjprs.2014.02.01
4 M. Koeva, M. Muneza, C. Gevaert, M. Gerke, and F. Nex: Survey Rev. **50** (2018) 361. https://doi.org/10.1080/0039 6265.2016.1268756
5 F. Nex and F. Remondino: Appl. Geomat. **5** (2014) 1. https://doi.org/10.1007/s12518-013-0120-x
6 S. Harwin and A. Lucieer: Remote Sens. **4** (2012) 1573. https://doi.org/10.3390/rs4061573
7 M. J. Westoby, J. Brasington, N. F. Glasser, M. J. Hambrey, and J. M. Reynolds: Geomorphology **170** (2012) 300. https://doi.org/10.1016/j.geomorph.2012.08.021
8 F. Neitzel and J. Klonowski: Int. Arch. Photogramm. Remote Sens. Spatial Inf. Sci. **38** (1/C22) (2011) 39.
9 G. Pajares: Photogramm. Eng. Remote Sens. **81** (2015) 281. https://doi.org/10.14358/PERS.81.4.281
10 M. Ibrahim: Int. J. Constr. Eng. Manage. **6** (2017) 235. https://doi.org/10.5923/j.ijcem.20170606.02
11 S. B. Lee, T. Kim, Y. J. Ahn, and J. O. Lee: Sens. Mate. **31** (2019) 3797. https://doi.org/10.18494/SAM.2019.2553
12 J. Travelletti, C. Delacourt, P. Allemand, J. P. Malet, J. Schmittbuhl, R. Toussaint, and M. Bastard: ISPRS J. Photogramm. Remote Sens. **70** (2012) 39. https://doi.org/10.1016/j.isprsjprs.2012.03.007
13 D. Turner, A. Lucieer, and S. de Jong: Remote Sens. **27** (2015) 1736. https://doi.org/10.1177/0309133313515293
14 U. Niethammer, M. R. James, S. Rothmund, J. Travelletti, and M. Joswig: M: Eng. Geol. **128** (2012) 2. https://doi.org/10.1016/j.enggeo.2011.03.012.
15 A. Lucieer, S. de Jong, and D. Turner: Prog. Phys. Geogr.: Earth Environ. **38** (2014) 97. https://doi.org/10.1177/0309133313515293
16 M. Yu, Y. Huang, J. Zhou, and L. Mao: Environ. Earth Sci. **76** (2017) 1. https://doi.org/10.1007/s12665-017-6860-x
17 M. M. Quédraogo, A. Degré, C. Debouche, and J. Lisein: Geomorphology **214** (2014) 339. https://doi.org/10.1016/j.geomorph.2014.02.016.

18 S. B. Lee, J. H. Won, K. Y. Jung, M. Song, and Y. J. Ahn: Sens. Mater. **32** (2020) 4347. https://doi.org/10.18494/SAM.2020.2973
19 H. H. Chris, M. W. Jordan, B. Owen, and M. A. Steve: J. Surv. Eng. **141** (2015). https://doi.org/10.1061/(ASCE)SU.1943-5428.0000138
20 S. Siebert and J. Teizer: Autom. Constr. **41** (2014) 1. https://doi.org/10.1016/j.autcon.2014.01.00
21 X. Wang, Z. Al-Shabbani, R. Sturgill, A. Kirk, and G. B. Dadi: TRB Annu. Meeting Promo Issue **2630** (2017) 1. https://doi.org/10.3141/2630-01
22 K. Julge, A. Ellmann, and R. Köök: Baltic J. Road Bridge Eng. **14** (2019) 1. https://doi.org/10.7250/bjrbe.2019-14.430
23 S. B. Lee, M. Song, S. Kim, and J. H. Won: Sens. Mater. **32** (2020) 3923. https://doi.org/10.18494/SAM.2020.2971

About the Authors

Suk Bae Lee received his B.E., M.S., and Ph.D. degrees from Sungkyunkwan University, Korea, in 1986, 1989, and 1997, respectively. From 1997 to 2003, he worked as a professor at Jeonju Vision College. Since 2004, he has been a professor at Gyeongsang National University, Korea. He was president of the Korean Society for Geospatial Information Science in 2018. His research interests are in geoid modeling, GNSS application, UAV photogrammetry, and smart construction. (sukbaelee@gnu.ac.kr)

Dongyeob Han received his B.S., M.S., and Ph.D. degrees from Seoul National University, Korea, in 1996, 1998, and 2007, respectively. Since 2007, he has worked as a professor at Chonnam National University, Korea. His research interests are in remote sensing, photogrammetry, and LiDAR. (hozilla@chonnam.ac.kr)

Mihwa Song received her B.S. degree from the Department of Radio Communication Engineering, Korea Maritime and Ocean University, Busan, Korea, in 2011, and her Ph.D. degree from the Department of Electrical and Computer Engineering, the University of Seoul, Seoul, Korea, in 2015. She is currently working as a deputy principal researcher at the Korea Expressway Corporation Research Institute, Hwaseong, South Korea. Her current research interests include wireless communications, cooperative communications, digital multimedia broadcast, cell broadcast service, and wireless emergency alert systems. (mihwa@ex.co.kr)